Phosphorus NMR Chemical Shifts with Self-Interaction Free, Gradient-Corrected DFT

Serguei Patchkovskii*,† and Tom Ziegler*,‡

Steacie Institute for Molecular Sciences, 100 Sussex Dr., Ottawa, Ontario, K1A 0R6 Canada, and Department of Chemistry, University of Calgary, 2500 University Dr. NW, Calgary, Alberta, T2N 1N4 Canada

Received: November 14, 2001

We examine the origin of the orbital localization requirement, commonly imposed on effective potential implementations of the Perdew−Zunger (PZ) self-interaction correction (SIC). We demonstrate that the condition arises because of the presence of irreducible off-diagonal Lagrangian multipliers in the coupled PZ eigenequations. Thus, this condition is essential for obtaining an energy-minimizing solution. Further, we report on an implementation of PZ SIC for the generalized gradient approximation (GGA) to the exchange-correlation energy within density functional theory (DFT). The implementation relies on the Krieger−Li−Iafrate (KLI) approximation to the optimized effective potential (OEP), simplifying the evaluation of molecular properties, such as the NMR chemical shifts. We examine several approaches toward incorporating the frozen core orbitals within the SIC−KLI−OEP scheme. To achieve an accurate description of both the energetic and magnetic properties, core orbitals must be included in the KLI potential on an equal footing with the valence orbitals. Implementation of the frozen core orbitals enables incorporation of relativistic effects via the quasirelativistic Pauli Hamiltonian. As the first application of the SIC−GGA approach, we examine ^{31}P NMR chemical shifts of 18 representative small molecules, as well as the previously reported C, H, N, O, and F SIC-LDA (local density approximation) test set. For C, N, O, and F NMR chemical shifts, SIC−GGA performs similarly to SIC−LDA, whereas a significant improvement is observed for hydrogen. Almost identical results, both for the chemical shifts and absolute shieldings, are obtained with different parent GGAs. For the ^{31}P test set, SIC−revPBE (revised Perdew−Burke−Ernzerhof functional of Zhang and Yang) leads to an root-mean-square (RMS) residual error of 23 ppm, compared to 54 ppm for its parent GGA, and 40 ppm for the SIC−VWN (Vosko−Wilk−Nusair) LDA functional. In particular, SIC−revPBE correctly reproduces the experimental trends in the PF_3−PCl_3−PBr_3−PI_3 series, which is described qualitatively incorrectly by VWN, revPBE, and SIC−VWN calculations. A similar improvement is observed for the ^{31}P shielding tensor components. The spurious self-interaction, in modern approximate DFT, appears to be a major, and so far largely overlooked, source of errors in calculations of the NMR shielding tensors.

1. Introduction

Because of a nuclear spin of $^1/_2$ and 100% natural abundance, phosphorus-31 is one of the easiest NMR nuclei to observe.[1] The interest in ^{31}P NMR has been increasing recently, as a result of its importance in studies of nucleic acids and other biological systems.[2] Both the isotropic NMR chemical shifts and the shielding tensor anisotropies[3,4] can be useful in such investigations. Structural interpretation of the NMR results in terms of simple, empirical structural increment rules is often possible for the lighter nuclei (H, C, N, O, and F). Such approaches have proven to be of only limited utility for ^{31}P chemical shifts.[5] Instead, the interpretation of phosphorus chemical shifts has benefited greatly from theoretical computations on the NMR shielding tensors.[5−16] Some recent examples of synergy between theory and experiment in phosphorus NMR include the determination of the NMR shielding tensors of the PI_4^+ cation[14] or the experimental confirmation[17] of the theoretically predicted[7,11] shielding tensor components of $M(CO)_5PR_3$ (M = Cr, Mo, or W) complexes. Multivariate analysis of theoretical ^{31}P chemical shifts was also used to devise simple empirical rules for ^{31}P substituent effects.[8,10,13] At the same time, achieving useful, uniform qualify in theoretical prediction of ^{31}P shielding tensors, across the whole range of phosphorus bonding environments, has proven more difficult than for the lighter nuclei.[6,7,10,14,16] Not only are ^{31}P NMR chemical shifts highly sensitive to the quality of the description of the electron correlation,[6,10,16] they are also influenced by relativistic effects.[7,11,14]

Classical correlated ab initio approaches to the NMR chemical shifts, such as MP2,[18−20] MP3,[21] CCSD,[22] CCSD(T),[23] CC2,[24] SOLO,[25] and MC−SCF,[26,27] can provide extremely accurate results for small, isolated systems. However, because of their computational complexity, such calculations are often impractical for larger molecules. With the development of density functional theory (DFT) approaches to the NMR chemical shifts,[28−35] DFT emerged as the method of choice for the prediction of the NMR parameters of systems with a large number of electrons, particularly where electron correlation is important. However, unlike classic ab initio approaches, approximate DFT does not provide a systematic way of improving the quality of the results. If the calculated NMR chemical shifts fail to follow the experimental trends, the only recourse is to try a different approximate functional, with no a priori reason to expect a better description of the NMR properties. For this reason, several simple semiempirical prescriptions have been

* To whom correspondence should be addressed. E-mail: Serguei.Patchkovskii@nrc.ca. E-mail: ziegler@ucalgary.ca.
† Steacie Institute for Molecular Sciences.
‡ University of Calgary.

10.1021/jp014184v CCC: $22.00
Published on Web 01/19/2002

proposed,[28,29,36,37] which often afford an improvement in the DFT magnetic properties. Two such prescriptions, by Malkin et al. ("SOS−DFPT"),[29,38] and by Wilson et al. ("WAH"),[36,37] have been particularly successful in solving many of the problematic cases in DFT NMR.[36,39,40] Devising a plausible theoretical justification for these prescriptions, as well as the formal consequences for the gauge dependence and the existence of the basis set limits within SOS−DFPT and WAH, has also attracted considerable attention.[16,28,29,36,41] Both SOS−DFPT and WAH start with the observation that DFT tends to underestimate the difference in the Kohn−Sham (KS) eigenvalues of the highest occupied molecular orbital (HOMO) and the lowest unoccupied molecular orbital (LUMO), compared to the experimental excitation energies. In SOS−DFPT, the orbital energy differences are "improved" by adding a suitable correction term in the denominator of the standard perturbational energy expressions for the NMR shielding tensors,[28,29] while the composition of the KS molecular orbitals is left unchanged. In the WAH approach,[36,42] the desired increase in the orbital energy differences is achieved by determining the KS orbitals from a hybrid DFT calculation, with a suitable fraction (typically 5%) of the exact Hartree−Fock exchange mixed in. Shielding tensors are then computed using standard, uncoupled DFT expressions. In both SOS−DFPT and WAH, the KS molecular orbitals are not self-consistent with the zeroth order Hamiltonian, employed (either explicitly or implicitly) in the property evaluation, with some undesirable consequences.[16,41] Unfortunately, both SOS−DFPT and WAH have been only partially successful in applications to the ^{31}P shieldings.[16,38] For this nucleus, WAH chemical shifts appear to be inferior to B3LYP DFT results,[16] and the (expensive) ab initio MP2 calculations were reported to be necessary for achieving uniformly accurate results.[6,10,16]

Recently, self-interaction corrected DFT (SIC−DFT), together with a simple local density approximation (LDA) exchange−correlation functional, was shown to offer a substantial improvement over the standard approximate functionals in calculations of the magnetic properties of C-, H-, N-, O-, and F-containing molecules and ions.[43] Because SIC−DFT relies on a physically well-defined contribution to the total energy and to the exchange−correlation potential, one might hope that a similar improvement is possible, also in cases where the more empirical schemes fail. In the present work, we augment the previously reported[43] SIC−DFT implementation in two aspects. First, the treatment of the Perdew−Zunger (PZ) self-interaction correction (SIC) is applied to gradient-corrected functionals. Further, the formalism is extended to allow a consistent treatment of the frozen core orbitals. The latter development allows self-consistent applications of the Pauli quasirelativistic Hamiltonian and, hence, applications to molecules, where relativistic effects may be important. The updated SIC−DFT approach is then applied to ^{31}P NMR chemical shifts and the shielding tensor component and shown to compare favorably with the best available calculations to date.

Section 2 of this paper briefly discusses the physical origin of the additional orbital localization step in SIC−OEP formulation, which is commonly imposed on semiintuitive grounds.[43,44] Section 3 outlines the implementation of the generalized gradient approximation (GGA) functionals and frozen core orbitals within the SIC−KLI−OEP scheme. Section 4 provides computational details. Sections 5 and 6 discuss respectively NMR results for the first main row nuclei and ^{31}P. Finally, section 7 provides the conclusions and outlines the directions for future work.

2. Orbital Localization and SIC−OEP

The theory behind the PZ SIC, optimized effective potentials (OEP), and the Krieger−Li−Iafrate (KLI) approximation to the OEP is discussed in detail elsewhere[45−53] and need not be restated. Therefore, we will only briefly recapitulate the key equations, essential for the practical implementation of SIC−KLI−OEP in a molecular DFT program. Within the PZ scheme, the total electronic energy of a system is given by (atomic units)[45]

$$E_{\mathrm{tot}}^{\mathrm{PZ}} = \sum_{\sigma=\alpha,\beta}\sum_{i=1}^{N_\sigma} n_{\sigma i}\left\langle \psi_{\sigma i}\left| -\frac{1}{2}\Delta \right| \psi_{\sigma i}\right\rangle + \frac{1}{2}\int \frac{\rho(\vec{r}_1)\,\rho(\vec{r}_2)}{r_{12}}\,\mathrm{d}\vec{r}_1\,\mathrm{d}\vec{r}_2 + \int v_{\mathrm{ext}}(\vec{r})\,\rho(\vec{r})\,\mathrm{d}\vec{r} + E_{\mathrm{xc}}^{\mathrm{approx}}[\rho_\alpha,\rho_\beta] - \sum_{\sigma=\alpha,\beta}\sum_{i}^{N_\sigma}\left\{\frac{1}{2}\int \frac{\tilde{\rho}_{\sigma i}(\vec{r}_1)\,\tilde{\rho}_{\sigma i}(\vec{r}_2)}{r_{12}}\,\mathrm{d}\vec{r}_1\,\mathrm{d}\vec{r}_2 + E_{\mathrm{xc}}^{\mathrm{approx}}[\tilde{\rho}_{\sigma i},0]\right\} \quad (1)$$

where $\psi_{\sigma i}$ are Kohn−Sham molecular orbitals (here assumed to be real), v_{ext} is the external potential, and $E_{\mathrm{xc}}^{\mathrm{approx}}$ is an approximate exchange-correlation energy functional. N_σ is the number of the (possibly partially) occupied spin-σ orbitals, whereas occupation numbers of the KS MOs are given by $n_{\sigma i}$. Spin-α and spin-β electron densities are given by ρ_α and ρ_β, whereas the total density is given by ρ. The last term in eq 1 represents the PZ energy correction, defined on the electron densities $\tilde{\rho}_{\sigma i}$ of localized orbitals $\tilde{\psi}_{\sigma i}$:

$$\tilde{\psi}_{\sigma i} = \sum_j U_{ji}^{\sigma}\psi_{\sigma j} \quad (2)$$

$$\tilde{\rho}_{\sigma i} = \tilde{n}_{\sigma i}|\tilde{\psi}_{\sigma i}|^2 \quad (3)$$

In eq 2, coefficients U_{ji}^{σ} define a unitary transformation

$$\sum_k U_{ki}^{\sigma}\,U_{kj}^{\sigma} = \delta_{ij} \quad (4)$$

and are chosen such that

$$U_{ji}^{\sigma} = 0 \quad \text{if} \quad n_{\sigma j} \neq \tilde{n}_{\sigma i} \quad (5a)$$

$$U_{ji}^{\sigma} = \delta_{ij} \quad \text{if} \quad i > N_\sigma \quad \text{or } j > N_\sigma \quad (5b)$$

The inverse transformation is then given by

$$\psi_{\sigma i} = \sum_k U_{ik}^{\sigma}\,\tilde{\psi}_{\sigma k} \quad (6)$$

The functional $E_{\mathrm{tot}}^{\mathrm{PZ}}$ has to be minimized, subject to the condition

$$\langle\psi_{\sigma i}|\psi_{\sigma j}\rangle = \delta_{ij} \quad (7a)$$

or, equivalently

$$\langle\tilde{\psi}_{\sigma i}|\tilde{\psi}_{\sigma j}\rangle = \delta_{ij} \quad (7b)$$

Except for the SIC, the functional $E_{\mathrm{tot}}^{\mathrm{PZ}}$ is invariant to unitary transformations between KS orbitals with the equal occupation numbers. Given the definition of U_{ji}^{σ} (eqs 4, 5), an *arbitrary*

choice of U will lead to the same energy, as long as the localized orbitals $\tilde{\psi}_{\sigma i}$ remain unchanged. It is therefore convenient to minimize the total energy functional with respect to the localized MOs $\tilde{\psi}$. Application of the standard variational techniques leads directly to the eigenequations

$$(\hat{f}_\sigma^{\mathrm{KS}} + v_{\sigma i}^{\mathrm{SIC}})\tilde{\psi}_{\sigma i} = \sum_j \lambda_{ij}^\sigma \tilde{\psi}_{\sigma j} \tag{8}$$

where the Lagrangian multipliers λ_{ij}^σ correspond to the constraints (7b) for the localized MOs i and j. Operators $\hat{f}_\sigma^{\mathrm{KS}}$ and $v_{\sigma i}^{\mathrm{SIC}}$ are given by

$$\hat{f}_\sigma^{\mathrm{KS}} = -\frac{1}{2}\hat{\Delta} + v_{\mathrm{ext}}(\vec{r}) + \int \frac{\rho(\vec{r}\,')}{|\vec{r} - \vec{r}\,'|}\,\mathrm{d}\vec{r}\,' + \frac{\delta E_{\mathrm{xc}}^{\mathrm{approx}}[\rho_\alpha,\rho_\beta]}{\delta\rho_\sigma} \tag{9}$$

$$v_{\sigma i}^{\mathrm{SIC}}(\vec{r}) = -\frac{\delta E_{\mathrm{xc}}^{\mathrm{approx}}[\tilde{\rho}_{\sigma i},0]}{\delta\tilde{\rho}_{\sigma i}} - \int \frac{\tilde{\rho}_{\sigma i}(\vec{r}\,')}{|\vec{r} - \vec{r}\,'|}\mathrm{d}\vec{r} \tag{10}$$

These eigenequations can be solved directly in an energy minimization approach.[46,47] In such implementations, the localization transformation (2) does not change the total energy, and it need not be considered.

Because the self-interaction contribution to the potential $v_{\sigma i}^{\mathrm{SIC}}$ is orbital-specific, the eigenequations (8) cannot be transformed to the diagonal, canonical form, without additional approximations. If an appropriately chosen universal effective potential (such as the OEP or the KLI approximation to the OEP) is substituted for $v_{\sigma i}^{\mathrm{SIC}}$, the eigenequations can be separated, giving

$$(\hat{f}_\sigma^{\mathrm{KS}} + v_\sigma^{\mathrm{KLI}})\psi'_{\sigma i} = \epsilon_{\sigma i}\psi'_{\sigma i} \tag{11}$$

where the eigenvalues $\epsilon_{\sigma i}$ are related to λ_{ij}^σ by a unitary transformation:

$$\epsilon_{\sigma i} = \sum_{kl} W_{ki}^\sigma\, \lambda_{kl}^\sigma\, W_{li}^\sigma \tag{12}$$

Because eq 1 provides complete freedom in the choice of the occupied MOs $\psi_{\sigma i}$ within the subspace spanned by the energy-minimizing orbitals $\tilde{\psi}_{\sigma i}$, the occupied canonical eigenorbitals $\psi'_{\sigma i}$ can be identified with the MOs $\psi_{\sigma i}$. The localization transformation U_{ij}^σ is then given simply by the eigenvectors of the nondiagonal Lagrangian multiplier matrix λ_{ij}^σ. The conditions, determining the transformation, can be derived by integrating the eigenequations (8) for $\tilde{\psi}_{\sigma i}$ and $\tilde{\psi}_{\sigma k}$ with respectively $\tilde{\psi}_{\sigma k}$ ad $\tilde{\psi}_{\sigma i}$, and subtracting[46,54,55]

$$\int \tilde{\psi}_{\sigma k}(\vec{r})[v_{\sigma i}^{\mathrm{SIC}}(\vec{r}) - v_{\sigma k}^{\mathrm{SIC}}(\vec{r})]\tilde{\psi}_{\sigma i}(\vec{r})\,\mathrm{d}\vec{r} = 0 \tag{13}$$

In practice, some approximation to the exact conditions, which does not require the (expensive) repeated evaluation of the self-interaction potentials $v_{\sigma i}^{\mathrm{SIC}}$ and $v_{\sigma k}^{\mathrm{SIC}}$, is usually employed.[43,44] In this respect, it is important to note that the condition (13) is satisfied exactly for any pair of orbitals, localized in spatially nonoverlapping regions, so that an arbitrary set of localized MOs automatically provides a good approximation to the exact conditions (13).

Finally, the proper effective potential approximation to the energy-minimizing solutions of the PZ eigenproblem (8) is given by the *localized* MOs $\tilde{\psi}$, rather than by the canonical orbitals $\psi_{\sigma i}$. It is then clear why the canonical MOs can be employed safely in atomic PZ calculations[45] but often lead to qualitatively incorrect results for molecular systems.[43,44,47] In atoms, the canonical MOs are necessarily similar to the energy-minimizing, localized MOs, so that the off-diagonal Lagrangian multipliers in eq 8 are small and can be ignored safely. In molecules, canonical MOs may extend over the whole system, making the off-diagonal contributions to λ_{ij}^σ more important.

3. Implementing Gradient-Corrected Functionals and Frozen Cores within SIC−KLI−OEP

In the SIC−KLI−OEP approximation, the effective potential v_σ^{KLI} is computed as a density-weighted average of the per-orbital SIC potentials:[50]

$$v_\sigma^{\mathrm{KLI}}(\vec{r}) = v_\sigma^{\mathrm{S}}(\vec{r}) + \rho_\sigma^{-1}(\vec{r}) \sum_{i=1}^{N_\sigma} \tilde{\rho}_{\sigma i}(\vec{r})(x_{\sigma i} - C_\sigma) \tag{14}$$

where

$$v_\sigma^{\mathrm{S}}(\vec{r}) = \rho_\sigma^{-1}(\vec{r}) \sum_{i=1}^{N_\sigma} \tilde{\rho}_{\sigma i}(\vec{r}) v_{\sigma i}^{\mathrm{SIC}}(\vec{r}) \tag{15}$$

The coefficients $x_{\sigma i}$ and C_σ are obtained by solving an auxiliary system of linear equations:

$$\sum_{j=1}^{N_\sigma} (\delta_{ij} n_{\sigma j} - M_{ij}^\sigma) x_{\sigma j} = \bar{v}_{\sigma i}^{\mathrm{S}} - \bar{v}_{\sigma i}^{\mathrm{SIC}},\ i = 1...N_\sigma \tag{16}$$

$$C_\sigma = \max(x_{\sigma i}) \tag{17}$$

(See ref 43 for the reasons behind this definition of the global potential shift parameter C_σ.) The auxiliary integrals M_{ij}^σ, $\bar{v}_{\sigma i}^{\mathrm{S}}$, and $\bar{v}_{\sigma i}^{\mathrm{SIC}}$, determined by numerical integration on a real-space grid, are given by

$$M_{ij}^\sigma = \int \frac{\tilde{\rho}_{\sigma i}(\vec{r})\tilde{\rho}_{\sigma j}(\vec{r})}{\rho_\sigma(\vec{r})}\,\mathrm{d}\vec{r} \tag{18}$$

$$\bar{v}_{\sigma i}^{\mathrm{S}} = \int \tilde{\rho}_{\sigma i}(\vec{r}) v_\sigma^{\mathrm{S}}(\vec{r})\,\mathrm{d}\vec{r} \tag{19}$$

$$\bar{v}_{\sigma i}^{\mathrm{SIC}} = \int \tilde{\rho}_{\sigma i}(\vec{r}) v_{\sigma i}^{\mathrm{SIC}}(\vec{r})\,\mathrm{d}\vec{r} \tag{20}$$

In our implementation, the Coulomb potentials of the individual localized MOs are computed using auxiliary fits to each orbital electron density.[43,56]

SIC−KLI−OEP and GGA Functionals. In our previous SIC−KLI−OEP implementation, as well as in most other molecular SIC codes[44,46,47,57] (but see refs 58 and 59), the approximate XC functional is restricted to the local density approximation form, such as X_α or VWN functionals. On the other hand, gradient-corrected functionals are usually superior to LDA in standard DFT calculations, particularly when chemical bonds are broken or formed.[60] GGA functionals also provide a much better approximation to the exact total electronic and atomization energies[60] and presumably reduce the self-interaction contribution in the energy.[61] Some of these improvements over LDA may be expected to carry over to a self-interaction corrected approach.

Incorporation of GGA functionals within the SIC−KLI−OEP approach requires the following changes to an existing LDA implementation:

1. Cartesian gradients of the localized per-orbital electron densities, $\tilde{\rho}_{\sigma i}$, need to be evaluated. The gradients are required

for evaluating the self-exchange contribution to the total energy ($E_{xc}^{approx}[\tilde{\rho}_{\sigma i}, 0]$ in eq 1) and the exchange-correlation part of the per-orbital SIC potential ($\delta E_{xc}^{approx}[\tilde{\rho}_{\sigma i}, 0]/\delta\tilde{\rho}_{\sigma i}$ in eq 10).

2. Cartesian second derivatives, of the per-orbital electron densities, are required for the exchange-correlation part of the per-orbital SIC potential.

These modifications can be incorporated into an existing SIC-LDA program with a minimal effort and at a moderate computational expense. In our implementation, a single-point SIC-GGA self-consistent calculation requires twice the time of a comparable SIC-LDA calculation.

SIC−KLI−OEP and Frozen Cores. In our previously reported SIC−KLI−OEP implementation,[43] all electrons are treated explicitly and are included in both the variational energy calculations and in the KLI−OEP potential evaluation. Although it is an acceptable choice for calculations involving only light nuclei, the all-electron approach leads to difficulties for heavier elements. In particular, the simplest quasirelativistic approach, employing the Pauli Hamiltonian, cannot be applied variationally in all-electron calculations with large basis sets, because of the danger of variational collapse of the core levels.[62] Additionally, the computational cost of the SIC−KLI−OEP is roughly proportional to the total number of variationally treated electrons in the system, making all-electron calculations on heavy elements relatively expensive. Finally, the need to approximate the rapidly varying densities of the localized core orbitals places a heavy demand on the quality of the auxiliary fit sets, which in turn may lead to numerical stability issues in practical calculations.

Similar issues arise in standard DFT calculations. In ADF (Amsterdam density functional) program,[56] they are solved by "freezing" the core orbitals at their atomic values. Frozen core orbitals on atom A in ADF are represented by an expansion over atom-centered Slater basis functions, with real tesseral harmonics[63] used for the angular parts of the orbitals:

$$\psi_{A,i}^{C}(\vec{r}) = \sum_{\mu} D_{\mu,i}^{A}\,\phi_{\mu}^{C}(\vec{r}) \qquad (21)$$

(An auxiliary minimal Slater basis set is used to ensure the orthogonality of the valence orbitals to the frozen core(s), see refs 56, 64, and 65 for details.) The coefficients $D_{\mu,i}^{A}$ are determined from atomic calculations and do not constitute an additional degree of freedom.

In atomic SIC studies, calculations employing canonical and localized MOs are known to lead to almost identical results for total energies and the orbital eigenvalues.[45,47] The same may be expected to hold true for the core orbitals in molecular calculations, so that application of the localization transformation (eq 2) appears unnecessary for the frozen core orbitals. As a result, the frozen core contribution to the self-interaction energy should cancel identically for all chemically meaningful energy differences. Thus, in the presence of the frozen core orbitals, the summation in eq 1 can be simply taken to run over the valence orbitals alone.

In standard DFT calculations, it is often acceptable to include only the outermost (ns, np, and (n − 1)d) atomic shells within the valence region and treat the remaining electrons with the frozen core approximation. However, in SIC calculations, the self-interaction energy is determined by the localized orbitals. If the core orbitals are frozen, and do not participate in the localization transformation (which would have introduced an undesirable additional degree of freedom), localized valence orbitals, derived from a frozen core calculation, are typically more extended, compared to an all-electron calculation. For this reason, two outermost electronic shells of each symmetry have to be included in the valence region in SIC calculations. An exception can be made for the first main row elements, where the compact, nodeless 1s orbital can be included within the frozen core, without substantially affecting the valence SIC energies.

The most straightforward approach toward evaluation of the frozen core contribution to the KLI potential, v_{σ}^{KLI}, is to explicitly include core orbitals in the average Slater potential (15) as well as in the KLI potential equilibration (the second term in eq 14). Because the potential shifts parameters $x_{\sigma i}$ are completely determined by the localized orbital densities $\tilde{\rho}_{\sigma i}$ (eqs 16−20), this does not introduce an additional degree of freedom. Moreover, because the orbital densities of the core orbitals remain frozen, their contributions to the average Slater potential, in the form of $\rho(\vec{r})v_{\sigma}^{S}(\vec{r})$, at grid points, can be precomputed and stored. We call this approach the "full" SIC−KLI−OEP treatment of the frozen core.

Calculation of the KLI shift parameters $x_{\sigma i}$, for the core orbitals, still requires that the core orbital densities are reevaluated on every SCF cycle. These densities are required for the evaluation of the integrals M_{ij}^{σ} (eq 18) for valence i and core j, $\bar{v}_{\sigma i}^{S}$ for the core orbitals, as well as in eq 14. In the spirit of the simplified SIC approach, proposed by Ullrich et al.,[57] it may appear attractive to neglect the (relatively expensive) equilibration contribution that is due to core orbitals, so that the summation in eqs 14 and 16 runs over the valence orbitals only. This is the "Slater" treatment of the frozen core. Finally, as the chemically relevant quantities may be expected to be unaffected by the fine details of the core potential, core contributions to the SIC−KLI−OEP potential can be neglected altogether, with summation in eqs 14−16 running over the valence orbitals only, and total density ρ_{σ} taken to exclude the core electron density. This is the "ignore" approximation for the SIC−KLI−OEP core potentials.

The "full" treatment can be expected to be the most accurate, but also the most expensive, approach to the KLI potential because of the frozen core orbitals. To strike the appropriate balance between the accuracy and computational expediency, we compare the three approaches to the all-electron treatment for Kohn−Sham orbital energies, atomization energies, and absolute NMR shielding constants of selected small molecules. For the orbital energies in CH_4, C_2H_4, and PF_3 (Table 1), the "full" treatment is clearly superior, with the average absolute relative error of just 0.6%. The distribution of the residual deviations in the "full" treatment is also uniform, with the largest relative deviation not exceeding 1.5% (for the virtual orbitals in PF_3). Ignoring the frozen core altogether also works well for the orbital energies, with an average relative error of 2.1%. As may be expected, the distribution of the relative errors is no longer uniform, with the larger errors observed for the core, virtual, and high-lying occupied orbitals. A similar behavior, of KLI−OEP orbital energies with respect to neglect of core orbital contributions, was observed previously.[66] Somewhat surprisingly, including the average Slater SIC potential for the core orbitals, but ignoring the equilibration contributions, is the worst possible approach. The average relative deviation from the all-electron results for this treatment is more than 20%, with some of the individual errors exceeding 40%. The complete failure of the "Slater" approach can be understood, given the relative magnitudes of the KLI shift constants $x_{\sigma i}$ for the core and valence orbitals. For third-row atoms, such as phosphorus, $x_{\sigma,1s}$ values are typically close to 1−4 Hartree (3.2 H for PH_3, using SIC−VWN), corresponding to an *up*ward shift of tens of

TABLE 1: Comparison of the Kohn−Sham Orbital Energies in Selected Molecules, within the All-Electron and Variants of the SIC−KLI−OEP Frozen Core Potential Treatment[a]

			treatment of the frozen core		
molecule	ϵ, eV	AE[b]	ignore[c]	slater[d]	full[e]
CH_4 (T_d)	$1a_1$ (core)	−276.92	−267.74	−295.54	−276.04
	$2a_1$ (occ)	−23.63	−23.49	−23.46	−23.64
	$1t_2$ (occ)	−16.00	−16.05	−16.00	−16.02
	$3a_1$ (virt)	−5.08	−5.06	−5.11	−5.09
	$2t_2$ (virt)	−3.45	−3.45	−3.53	−3.44
C_2H_4 (D_{2h})	$1a_{1g}$ (core)	−276.81	−267.61	−296.09	−275.88
	$1b_{3u}$ (core)	−276.79	−267.61	−296.09	−275.88
	$2a_{1g}$ (occ)	−24.59	−24.40	−24.26	−24.61
	$2b_{3u}$ (occ)	−19.92	−19.81	−19.68	−19.95
	$1b_{2u}$ (occ)	−17.21	−17.25	−17.05	−17.25
	$3a_{1g}$ (occ)	−15.96	−16.01	−15.97	−15.98
	$1b_{1g}$ (occ)	−14.22	−14.25	−14.07	−14.26
	$1b_{1u}$ (occ)	−12.46	−12.52	−12.52	−12.47
	$1b_{2g}$ (virt)	−6.45	−6.50	−6.70	−6.46
	$4a_{1g}$ (virt)	−4.14	−4.11	−4.02	−4.16
PF_3 (C_{3v})	$1a_1$ (core)	−2093.69	−2071.76	−2142.87	−2088.27
	$1e_1$ (core)	−668.91	−656.46	−698.17	−666.74
	$2a_1$ (core)	−668.91	−656.46	−698.17	−666.74
	$3a_1$ (occ)	−184.20	−182.89	−193.22	−184.10
	$2e_1$ (occ)	−135.88	−135.43	−145.71	−135.76
	$4a_1$ (occ)	−135.74	−135.29	−145.52	−135.62
	$5a_1$ (occ)	−37.37	−37.63	−33.33	−37.35
	$3e_1$ (occ)	−36.32	−36.53	−32.17	−36.28
	$6a_1$ (occ)	−22.35	−22.88	−19.49	−22.44
	$4e_1$ (occ)	−19.28	−19.99	−15.99	−19.40
	$7a_1$ (occ)	−18.10	−18.84	−14.87	−18.24
	$5e_1$ (occ)	−17.30	−18.09	−13.72	−17.44
	$6e_1$ (occ)	−16.49	−17.29	−12.98	−16.64
	$1a_2$ (occ)	−16.22	−17.02	−12.70	−16.36
	$8a_1$ (occ)	−13.85	−14.30	−11.87	−13.94
	$7e_1$ (virt)	−6.90	−7.37	−5.02	−6.99
	$9a_1$ (virt)	−4.77	−5.28	−2.78	−4.84
average relative absolute error, percent			2.1	21.1	0.6

[a] Using TZ2P basis sets, optimized BP86 geometries, and nonrelativistic Hamiltonian. [b] All-electron calculations. [c] No SIC potential because of the core orbitals. [d] Core orbitals contribute to the average Slater potential (eq 15) but do not participate in the KLI "potential stitching" (eq 14). [e] Frozen core orbitals are treated identically to the localized valence orbitals.

TABLE 2: Comparison of the Atomization Energies, in kcal/mol, of Selected Molecules, within the All-Electron and Variants of the SIC−KLI−OEP Frozen Core Potential Treatment[a]

		treatment of the frozen core		
molecule	AE[b]	ignore[c]	slater[d]	full[e]
CH_4	467.65	472.39	470.66	471.62
C_2H_4	627.90	636.99	634.00	635.39
N_2	239.23	241.15	234.22	241.29
PH_3	330.61	330.05	288.07	330.67
PF_3	416.17	438.23	422.31	435.32
average relative absolute error, percent		1.8	3.6	1.5

[a] Using TZ2P basis sets, optimized BP86 geometries, and nonrelativistic Hamiltonian. [b] All-electron calculations. [c] No SIC potential because of the core orbitals. [d] Core orbitals contribute to the average Slater potential (eq 15) but do not participate in the KLI "potential stitching" (eq 14). [e] Frozen core orbitals are treated identically to the localized valence orbitals.

TABLE 3: Comparison of Nonrelativistic Absolute Shielding Constants (in ppm) for Selected Molecules, within the All-Electron and Variants of the SIC−KLI−OEP Frozen Core Potential Treatment[a]

			treatment of the frozen core		
molecule	nucleus	AE[b]	ignore[c]	slater[d]	full[e]
CH_4	C	191.5	191.2	178.5	191.2
	H	30.61	30.66	29.85	30.65
C_2H_4	C	58.0	58.7	−4.6	59.8
	H	25.11	25.20	23.93	25.20
N_2	N	−73.8	−71.0	−173.8	−68.6
PH_3	P	569.6	568.4	486.0	567.6
	H	28.45	28.43	26.45	28.44
PF_3	P	149.7	171.4	−49.4	150.2
	F	198.3	212.1	92.0	202.7
average relative absolute error, percent			3.1	51.8	1.5

[a] Using TZ2P basis sets, optimized BP86 geometries, and nonrelativistic Hamiltonian. [b] All-electron calculations. [c] No SIC potential because of the core orbitals. [d] Core orbitals contribute to the average Slater potential (eq 15) but do not participate in the KLI "potential stitching" (eq 14). [e] Frozen core orbitals are treated identically to the localized valence orbitals.

electron volts in the core orbital energies. When this contribution is excluded, as in the "Slater" frozen core treatment, core orbitals become excessively stable. Simultaneously, high-lying occupied MOs and virtual MOs are destabilized, compared to all-electron calculations. Thus, the "Slater" treatment appears to be unsuitable for practical calculations and need not be discussed any further.

Compared to the orbital energies, atomization energies (Table 2) are less sensitive to the choice of the frozen core potential treatment. Very similar residual errors are found for the full treatment and by ignoring core orbitals altogether. Finally, for the NMR absolute shielding constants (Table 3), the "full" treatment is, again, superior to ignoring the SIC potential of the core orbitals. The average errors are respectively 1.5% for the full treatment and 3.0% for the "ignore" approach, with the "ignore" approach showing substantial deviations from all-electron results for some molecules (PF_3). Overall, it appears that only the "full" treatment of the frozen core orbitals leads to an acceptable description of molecular properties.

One technical aspect of the implementation of the frozen core KLI potentials, worth mentioning, is the evaluation of the Coulomb potential that is due to the frozen core orbitals. In ADF, the Coulomb potential, of the valence electron density, is determined by a secondary fitting of the electron density.[56,64,65] For the core orbitals, where the total core density is necessarily spherically symmetric, the potential is determined through one-dimensional numerical integration. Neither approach is appealing for the evaluation of the Coulomb potentials of the individual core orbitals. The numerical integration approach is not appropriate, because of the loss of spherical symmetry for the individual orbitals. The secondary fitting technique can, in principle, be adapted to the core orbitals. However, this would necessitate the inclusion of a large number of steep, high-angular momentum functions in the fitting basis set, thus largely negating computational advantages of the frozen core approximation.

At the same time, the frozen core orbitals (21) are, by definition, expressed in terms of basis functions, centered on the same atom. The corresponding orbital densities can then be expressed as a sum over auxiliary Slater product functions, centered on the same atom:

$$\rho^{C}_{A,i}(\vec{r}) = \sum_{\mu\nu} D^{A}_{\mu,i} D^{A}_{\nu,i} \phi^{C}_{\mu}(\vec{r})\phi^{C}_{\nu}(\vec{r}) = \sum_{\lambda}\{\sum_{\mu\nu} D^{A}_{\mu,i} D^{A}_{\nu,i} E_{\lambda,\mu\nu}\}\chi^{C}_{\lambda}(\vec{r}) \quad (22)$$

If the core basis functions ϕ^{C}_{μ} and ϕ^{C}_{ν} are determined by respectively quantum numbers (n_μ, l_μ, m_μ) and (n_ν, l_μ, m_μ) (only functions with the identical orbital and magnetic quantum numbers l and m may contribute to the same core orbital), the

corresponding product functions must have quantum numbers $n_\lambda = n_\mu + n_\nu - 1$, $l_\lambda = 0, 2, ..., 2l_\mu$, and $n_\lambda = -2|m_\mu|, 0, +|m_\mu|$. The orbital exponent ζ_λ is always the sum of the orbital exponents ζ_μ and ζ_ν. The coupling coefficients $E_{\lambda,\nu\nu}$ may be expressed in terms of 3*J* symbols.[67] Once the expansion (22) of the core orbital densities, in terms of auxiliary Slater-type product functions, is determined, standard techniques[56,64,65] can be used to compute per-orbital Coulomb potential. Thus, in effect, we generate the optimal, exact fit set for every individual core orbital.

4. Computational Details

All calculations are based on DFT[60,62,68] and were performed with the ADF program package,[56,64,65,69] using Cartesian space numerical integration[70] and analytical gradients for the geometry optimization.[71] For the C, H, N, O, and F data set, calculations were performed at the previously reported[43] optimized geometries. For the phosphorus data set, molecular geometries were optimized using the revPBE[72−74] GGA functional and ADF standard basis set IV of TZP quality in the valence region of main-group elements,[75] with *n*s, *n*p, and (*n* − 1)d (if present) electron shells included within the valence part. Scalar relativistic effects, on the molecular geometry, were included within the quasirelativistic framework[76] employing relativistic frozen core potentials, in conjunction with the first-order Pauli Hamiltonian. The final optimized geometries are provided as Supporting Information. For PH_3, PF_3, PCl_3, PBr_3, and PI_3, which are described poorly by GGA functionals,[7,11,16] experimental geometries[77,78] were also used in NMR calculations.

Calculations involving the SIC functionals were performed with a modified version of ADF. The SIC−KLI−OEP implementation supports both local and generalized gradient approximation (GGA) functionals of the spin-density as E_{xc}^{approx} in eq 1. Frozen atomic core orbitals are also supported within a SIC calculation, as described above. The SIC correction was applied self-consistently, with the Foster-Boys[79,80] localization procedure used to obtain approximate solutions for the variational conditions (13).

Calculations of the NMR shielding tensors employed gauge-including atomic orbitals (GIAOs),[81−83] using the implementation of Schreckenbach and Ziegler.[31,35] Basis set with 3x(*n*s), 3x(*n*p), and 2x(*n*d) functions was used on hydrogen atoms. For the NMR calculations on molecules from the C, H, N, O, and F set, the previously reported[43] all-electron Slater basis sets of TZ2P quality, containing 5x(*n*s), 3x(*n*p), 2x(*n*d), and 2x(*n*f) basis functions, was used. These calculations employed a nonrelativistic Hamiltonian.

NMR calculations, on molecules from the phosphorus data set, employed a scalar quasirelativistic Pauli Hamiltonian, together with a Slater basis set of TZ2P quality in the valence region. Frozen 1s cores were used on C, N, O, F, P, Si, and Cl. Chromium and bromine basis sets employed 2p frozen cores, whereas a 3p frozen core was used on iodine. From the previous experience,[31,84] these basis sets are approaching saturation for calculations of NMR chemical shifts. In all cases, the auxiliary fitting sets were optimized to reproduce atomic orbital densities to machine accuracy.[85] These basis sets are included in the Supporting Information.

All calculations were performed with Vosko−Wilk−Nusair (VWN)[86] LDA, BP86,[87,88] and revPBE[72,73] GGA functionals. These functionals were applied self-consistently, both in standard DFT calculations and within the SIC−KLI−OEP program.

5. SIC-GGA for NMR Chemical Shifts of C, H, N, O, and F

Before discussing the NMR chemical shift results for ^{31}P, it is instructive to examine the performance of SIC−GGA functionals for the previously studied[43] C, H, N, O, and F data set. For these nuclei, SIC−LDA already provides qualitative improvement over standard LDA and GGA functionals. The statistical evaluation of the results, for this reference set, is given in Table 4. The individual chemical shifts are provided in Table S2 of the Supporting Information, whereas the reference isotropic shieldings (see ref 43 for details of the statistical evaluation procedure) are given in Table S3. As can be seen from the results, the two SIC−GGA functionals, examined presently (SIC−BP86 and SIC−revPBE), lead to essentially identical results for the NMR chemical shifts. For this reason, only SIC−revPBE results will be discussed from now on.

On average, SIC−GGA results for C, N, and F present a modest improvement over those for SIC−LDA. For carbon, the rms error decreases from 7.1 (SIC−VWN) to 6.5 ppm (SIC−revPBE) compared to 6.3 ppm for revPBE GGA itself. For nitrogen, SIC−VWN error of 21.3 ppm is reduced to 17.7 ppm with SIC−revPBE. The parent GGA functional (revPBE) leads to the rms error of 68.2 ppm for this nucleus. For fluorine, SIC−revPBE leads to 13.1 ppm rms error, whereas SIC−VWN and revPBE give respectively 14.5 and 18.7 ppm. Individual SIC−VWN and SIC−revPBE chemical shifts, computed for C, N, and F nuclei, are also quite similar.

Oxygen NMR chemical shifts are more interesting: the SIC−revPBE rms error for this nucleus is dominated by the chemical shift of the terminal oxygen atoms in ozone. This chemical shift is too positive with LDA (1830 ppm) and revPBE (1754 ppm) compared to the experimental value of 1630 ppm. At the same time, all self-interaction corrected functionals predict chemical shift values for the terminal oxygen, which are too shielded: 1477 ppm for SIC−VWN and 1369 ppm for SIC−revPBE. This, in turn, leads to SIC−revPBE rms error of 80 ppm compared to SIC−VWN error of 70 ppm. In this respect, it is interesting to note that highly correlated ab initio techniques also predict the terminal oxygen in ozone to be too shielded compared to the experiment.[89] Thus, MCSCF−GIAO predicts chemical shift of about 1461 ppm,[90] whereas CCSD(T)−GIAO finds 1516 ppm[23] for this nucleus. Given the experimental error bar of 170 ppm cited for this chemical shift, it appears reasonable to exclude it from the statistical evaluation of the results. Once ozone is excluded, both SIC−VWN and SIC−revPBE rms errors decrease to respectively 53 and 45 ppm, in comparison to the revPBE error of 104 ppm for the same restricted subset.

For ^1H chemical shifts, SIC−VWN fails to improve the results compared to the parent VWN LDA functional (rms error of 0.44 vs 0.46 ppm). As a consequence, SIC−VWN ^1H chemical shifts are not competitive with standard GGA results[91] (revPBE rms error for the same data set is 0.32 ppm). However, when SIC is combined with a gradient-corrected approximate exchange-correlation functional, the rms error improves dramatically, to 0.22 ppm in the case of SIC-revPBE. This residual error is obtained *without scaling* the results and compares favorably to the best *scaled* results for ^1H chemical shifts, obtained with standard functionals.[91] A large fraction of the overall improvement is obtained for the proton chemical shifts in small molecules, with the hydrogen nuclei attached directly to an atom carrying electron lone pairs or participating in a multiple bond (HOF, H_2O, H_2O_2, HCH, and NH_3).

TABLE 4: Statistical Evaluation of the SIC−VWN, SIC−BP86, and SIC−revPBE Results for Isotropic NMR Chemical Shifts of C, H, N, O, and F Containing Molecules, in Comparison with the Parent Functionals

	C	H	N	O	(O)[a]	F
number of data points	49	19	18	18	(16)	12
range expt values, ppm	231.9	12.2	692.2	1647.0	(904.0)	703.7
			VWN			
average abs. error, ppm	7.4	0.36	39.1	106.7	(93.1)	20.7
RMS error, ppm	9.2	0.46	86.3	138.7	(135.3)	27.7
RMS/range, percent	4.9	3.7	12.4	8.4	(15.0)	3.9
correlation slope	1.095	1.120	1.316	1.254	(1.347)	1.119
			BP86			
average abs. error, ppm	4.7	0.26	31.3	83.6	(74.2)	14.8
RMS error, ppm	6.6	0.32	69.2	106.7	(105.4)	20.7
RMS/range, percent	2.8	2.6	9.9	6.4	(11.7)	2.9
correlation slope	1.036	1.073	1.237	1.184	(1.256)	1.074
			revPBE			
average abs. error, ppm	4.2	0.25	30.9	80.4	(72.7)	13.5
RMS error, ppm	6.3	0.32	68.2	103.8	(103.6)	18.7
RMS/range, percent	2.7	2.6	9.9	6.3	(11.5)	2.7
correlation slope	1.023	1.071	1.224	1.173	(1.245)	1.064
			SIC−VWN			
average abs. error, ppm	5.0	0.27	13.6	46.1	(41.4)	11.3
RMS error, ppm	7.1	0.44	21.3	70.1	(53.1)	14.5
RMS/range, percent	3.0	3.6	3.0	4.2	(5.9)	2.1
correlation slope	1.035	1.075	1.032	0.960	(1.078)	1.073
			SIC−BP86			
average abs. error, ppm	5.3	0.17	12.8	53.3	(37.1)	9.6
RMS error, ppm	6.6	0.24	17.0	79.4	(45.6)	12.3
RMS/range, percent	2.8	1.9	2.5	4.8	(5.0)	1.7
correlation slope	0.963	1.022	0.937	0.867	(0.979)	0.952
			SIC-revPBE			
average abs. error, ppm	5.1	0.16	13.5	54.0	(37.4)	10.1
RMS error, ppm	6.5	0.22	17.7	79.8	(45.1)	13.1
RMS/range, percent	2.8	1.6	2.6	4.8	(5.0)	1.9
correlation slope	0.965	1.025	0.937	0.865	(0.979)	0.947

[a] Excluding ozone.

When comparing the results from calculations of the NMR chemical shifts, at equilibrium molecular geometries, to experiment, one should always keep in mind the zero-point motion and thermal averaging effects. Relative to the chemical shift range, such effects are particularly large for hydrogen.[92−94] In extreme cases, zero-point vibrational corrections to the ^{1}H absolute shieldings may amount to +0.50/−0.70 ppm.[94] Therefore, the 0.22 ppm rms error, obtained for the ^{1}H NMR chemical shifts with SIC−revPBE, must, to a large extent, arise from a fortuitous cancellation of errors. The same observation applies to other theoretical approaches, which utilize solely the equilibrium molecular geometries.[94]

Overall, SIC−GGA functionals provide a modest, but significant, improvement to the calculated NMR chemical shifts for the first main-row elements (C, N, O, and F) compared to those for SIC−VWN. For hydrogen, where SIC−VWN failed to improve the results, compared to VWN itself, SIC-GGA functionals hold a substantial advantage.

6. SIC−GGA for NMR Chemical Shifts of ^{31}P

For ^{31}P, we adopted the reference set of van Wüllen,[16] which has been studied with several DFT (BP86 and B3LYP), ab initio (HF and MP2), and empirically adjusted (WAH) approaches. This data set was augmented with PCl_3, PI_3, and P_2H_2, which are known to present difficulties in standard DFT and ab initio calculations.[6,15,38] Because the experimental ^{31}P reference (85% phosphoric acid) is not suitable for direct theoretical comparisons, we follow the procedure of van Wüllen[16] for calculation of the ^{31}P chemical shifts. Calculated absolute shieldings are converted to the NMR chemical shifts, such that the experimental gas-phase chemical shift of PH_3 (−266.1 ppm[95]) is reproduced exactly, i.e

$$\delta(X) = \sigma(PH_3,\text{calcd}) - \sigma(X) - 266.1\ \text{ppm} \qquad (23)$$

Calculated SIC−VWN and SIC−revPBE NMR chemical shifts are collected in Table 5, in comparison with the parent XC functionals (VWN and revPBE) and the experiment. The correlations between the experimental and calculated chemical shifts, for these four approaches, are illustrated in Figures 1−4. Where available in the literature, results obtained with empirically corrected WAH technique,[36,42] B3LYP hybrid functional, and ab initio MP2 are given for comparison.

At this point, we should emphasize that the effects of a gradient-corrected functional and of the SIC on the absolute NMR shielding are not additive. As an example, for PH_3 at the experimental geometry, we calculate ^{31}P isotropic shieldings σ of 590.6 (VWN) and 578.8 ppm (SIC−VWN), so that accounting for the self-interaction error *reduces* the absolute shielding by 12 ppm. At the same time, the corresponding revPBE and SIC−revPBE σ values are 584.0 and 592.2 ppm, so that, in this case, the absolute shielding is *increased* by taking self-interaction into account. Given that the phosphorus basis set, used in this study, is far from saturation in the core region, the excellent agreement of the SIC−revPBE absolute shielding with the experiment (594.45 ± 0.63[95]) should be treated as fortuitous.

As was documented previously,[7,16] optimized DFT bond lengths in PF_3, PCl_3, PBr_3, and PI_3 show large deviations from the experiment and are therefore unsuitable[12] for NMR chemical

TABLE 5: Calculated SIC−DFT ^{31}P NMR Chemical Shifts (in ppm), in Comparison with Other Theoretical Techniques and the Experiment

molecule	expt.[a]	VWN[b]	revPBE[b]	SIC−VWN[b]	SIC−revPBE[b]	WAH[c]	B3LYP[c]	MP2[c]
P_4	−552.	−472.3	−487.2	−508.2	−526.3	−512.9	−532.5	−549.1
PN	275.	406.4	347.3	318.8	270.8	307.8	342.7	202.2
PH_3[d]	−266.	−266.1	−266.1	−266.1	−266.1	−266.1	−266.1	−266.1
PH_3		(−256.2)	(−256.4)	(−257.9)	(−259.1)			
PF_3[d]	106.	163.4	120.9	127.0	108.5	95.8	115.7	109.7
PF_3		(201.2)	(158.2)	(158.1)	(137.7)			
PCl_3[d]	217.	312.7	255.9	249.4	200.4	222.0	259.6	224.9
PCl_3		(387.6)	(327.1)	(314.5)	(257.3)			
PBr_3[d]	226.	372.2	309.3	277.9	198.4			
PBr_3		(493.2)	(423.1)	(377.5)	(281.1)			
PI_3[d]	176.	387.1	309.2	243.3	143.4			
PI_3		(524.5)	(440.2)	(353.1)	(229.5)			
$Si(PH_2)_4$	−205.	−167.4	−194.5	−197.8	−218.3	−225.1	−226.0	−243.1
$P(CH_3)_3$	−63.	−8.6	−36.0	−35.7	−60.9	−73.2	−58.4	−75.0
$P(iso\text{-}C_3H_7)_3$	20.	103.7	60.9	77.0	42.6	11.4	27.3	10.6
$OP(CH_3)_3$	36.	72.7	34.6	45.6	24.8	−4.0	14.0	18.7
$P(OCH_3)_3$	140.	209.1	166.9	199.7	173.2	100.1	128.4	129.3
$OP(OCH_3)_3$	0.	70.6	33.6	39.9	28.0	−33.7	−16.7	−5.0
PF_6^{1-}	−145.	−56.1	−86.2	−93.3	−102.1	−121.1	−120.2	−119.5
PH_4^{1+}	−105.	−99.1	−114.0	−123.3	−130.5	−153.2	−128.9	−127.6
$P(CH_3)_4^{1+}$	25.	96.0	50.3	57.3	30.1	1.8	22.1	12.5
$Cr(CO)_5PH_3$	−130.	−111.3	−121.2	−109.5	−118.2	−149.8	−123.0	−176.7
trans-"P_2H_2"[e]	(494.)	678.1	587.3	540.3	456.2			735.[f]
cis-"P_2H_2"		652.3	565.2	516.2	436.0			

[a] Experimental values for the ^{31}P chemical shifts in PBr_3 and PI_3 are from ref 104 (somewhat different values are available in ref 105). "P_2H_2" (1,2-bis(tri-tertbutylphenyl)diphosphene) is from ref 99. The rest of the experimental values are cited from ref 16. [b] This work. [c] Cited from ref 16. [d] Experimental geometry. [e] The experimental value corresponds to Ar − P = P − Ar, with Ar = tris-*tert*-butylphenyl.[99] Calculations were performed on P_2H_2. [f] Cited from ref 6.

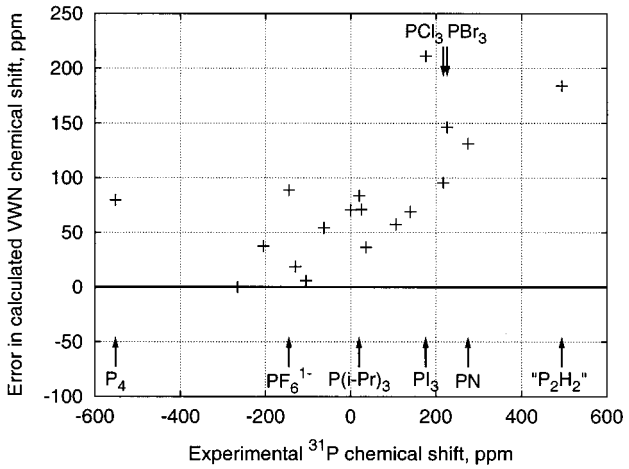

Figure 1. Residual errors in the calculated VWN ^{31}P NMR chemical shifts.

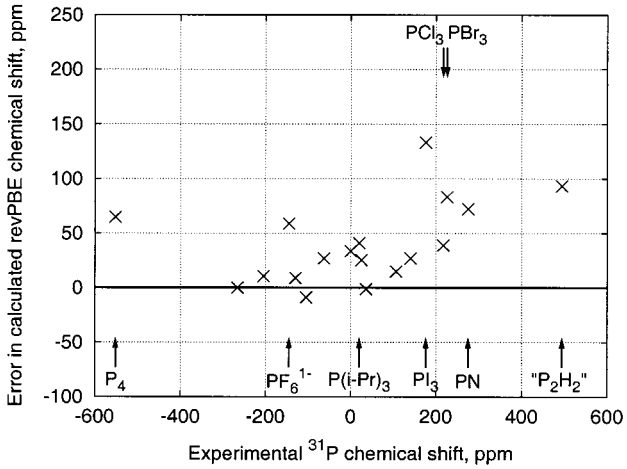

Figure 2. Residual errors in the calculated revPBE ^{31}P NMR chemical shifts.

shift calculations. The differences in the absolute shieldings at the optimized and experimental geometries are particularly severe for PI_3, where the shieldings of two structures differ by 86 (SIC−revPBE) to 137 (VWN) ppm. This should be compared to the total experimental chemical shift range of 1046 ppm, for this reference set. Substantial differences between experimental and optimized geometries are obtained for PF_3, PCl_3, and PBr_3 as well (see Table 5). For this reason, all comparisons involving chemical shifts of phosphorus (III) halides were performed at the experimental geometries. The differences in the absolute ^{31}P shielding of PH_3 between the experimental and optimized geometry are much less pronounced (9.8 ppm for VWN and 6.9 ppm for SIC−revPBE). At the same time, any deficiency in the calculated absolute shielding in this molecule gets amplified disproportionately in the final average error. For this reason, the experimental geometry was used for PH_3 as well.

As reported previously,[16] ^{31}P chemical shifts calculated with standard LDA and GGA functionals are systematically too deshielded. Larger errors are obtained for strongly deshielded molecules ("P_2H_2", PN, PCl_3, PBr_3, and PI_3), so that the correlation slope is far from 1.0 (Figures 1 and 2). For 13 (out of 18) molecules, VWN results deviate from experiment by more than 52 ppm or 5% of the experimental range. For revPBE, six of the calculated chemical shifts (P_4, PF_6^-, PI_3, PBr_3, PN, and "P_2H_2") are outside of the 5% relative error range. The largest deviations from experiment are seen for PI_3 (VWN, 387; revPBE, 309; expt, 176 ppm) and PN (VWN, 406; revPBE, 347; expt, 275 ppm). Once the self-interaction error is accounted for, the deviations from experiment drop substantially (Figures 3 and 4). For SIC−VWN, only three molecules (PI_3, $P(OCH_3)_3$, and $P(iso\text{-}C_3H_7)_3$) show deviations in excess of 52 ppm (two more ^{31}P chemical shifts, in PBr_3 and PF_6^-, are too deshielded by 52 ppm). With SIC−revPBE, all calculated ^{31}P chemical

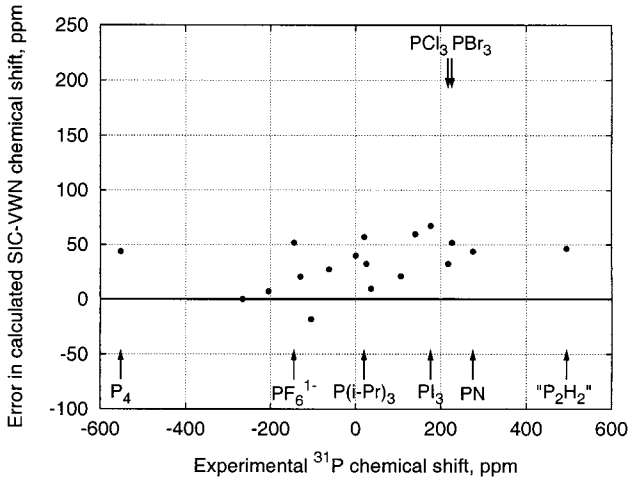

Figure 3. Residual errors in the calculated SIC−VWN ^{31}P NMR chemical shifts.

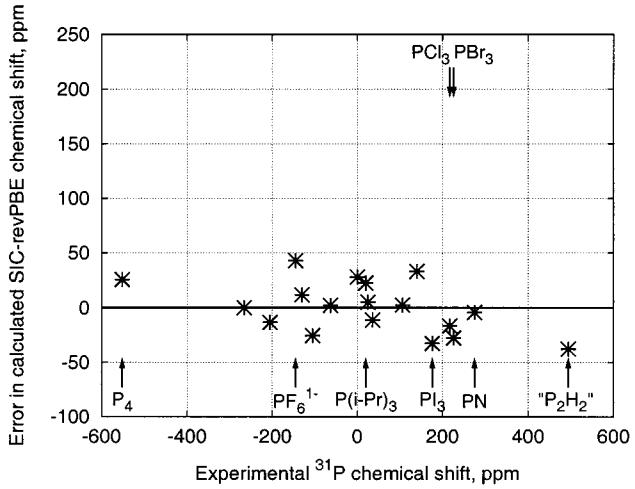

Figure 4. Residual errors in the calculated SIC−revPBE ^{31}P NMR chemical shifts.

shifts fall within the 52 ppm error band, so that both "simple" and "difficult" cases are treated uniformly. The correlation slope is also much improved for both self-interaction corrected functionals (Table 6).

These visual observations are corroborated by the statistical analysis of the calculated chemical shifts, given in Table 6. For the complete reference set of 18 ^{31}P chemical shifts, the VWN rms error of 98 ppm is reduced to 40 ppm with SIC−VWN. For the gradient-corrected revPBE functional, the rms residual error is reduced from 54 (revPBE) to 23 ppm (SIC−revPBE), or just 2.2% of the total experimental range for this data set. Excluding the three worst outliers (PI_3, PBr_3, and "P_2H_2") reduces VWN and revPBE rms errors by one-third, to respectively 69 and 36 ppm (the bottom half of Table 6). Because these molecules do not present any particular difficulty for self-interaction corrected functionals, SIC−VWN and SIC−revPBE rms errors remain almost the same (SIC−VWN, 36 ppm; SIC−revPBE, 21 ppm).

It is instructive to examine the performance of the SIC functionals for the series of phosphorus(III) halides PX_3 (X = F, Cl, Br, and I) in a little more detail. The experimental chemical shifts curve (Figure 5) exhibits a characteristic "hump", with the most deshielded values observed for the two middle members of the series (PCl_3, 217 ppm; PBr_3, 226 ppm). At the same time, the two extreme members of the series are more shielded (PF_3, 106 ppm; PI_3, 176 ppm). These trends are reproduced qualitatively incorrectly by both local (VWN) and gradient-corrected (revPBE) functionals. In either case, the phosphorus nucleus is predicted to grow progressively more deshielded for heavier halogen substituents (the two upper curves in Figure 5). Once the self-interaction error is accounted for, even the simple SIC−VWN functional leads to a qualitatively correct trend, with PI_3 being more shielded than PBr_3. Finally, when the SIC is combined with a GGA functional (the bottom curve in Figure 5), calculated NMR chemical shifts come into an almost quantitative agreement with experiment.

For other halogen-substituted series, such as HX,[96,97] CX_4,[98] PX_4^+,[14] or POX_3,[15] the nonmonotonic dependence of the chemical shifts, on the halogen substituent, has been rationalized in term of increasing spin−orbit (SO) effects for heavier halogen atoms. Although it appears that the SO contributions are much less important for phosphorus(III), compared to those for phosphorus(V),[15] it might have be interesting to examine the effect of the spin−orbit corrections on the calculated SIC-DFT chemical shifts in the PX_3 series as well. Unfortunately, our current program does not support spin−orbit calculations within the SIC approach. Such corrections are known to be sensitive to the structure of the core tails of the valence orbitals, close to the heavy nucleus.[15] Because this region is heavily affected by the SIC,[45−47] SIC and spin−orbit corrections cannot be expected to be additive. Therefore, the question of the relative importance of the SIC and the spin−orbit corrections, for the NMR chemical shifts of the PX_3 series, will have to remain open for future investigations.

In addition to judging SIC functionals, relative to the standard LDA and GGA DFT approaches, it is also important to examine their performance in comparison to other theoretical techniques. For the smaller, 15 point data set, ^{31}P NMR chemical shifts, calculated using other DFT and ab initio approaches, are available in the literature.[16] Table 6 provides a statistical evaluation of these literature results. The lowest rms error is obtained for the hybrid B3LYP DFT approach (25 ppm), closely followed by ab initio MP2 (27 ppm) and the empirically corrected WAH approach (28 ppm). Other DFT and noncorrelated ab initio approaches perform significantly worse for the ^{31}P NMR chemical shifts.[6,16] These average errors are significantly higher that the SIC−revPBE result for the same data set (21 ppm), which also exhibits a correlation slope closer to unity and the smallest intercept among all methods. Once the "difficult" molecules are included in the reference set, the difference between SIC-GGA, and other techniques, would likely increase. Thus, the MP2 ^{31}P chemical shift of 735 ppm has been reported for P_2H_2,[6] 241 ppm above the experimental value of 494 ppm (measured for an aryl-substituted derivative[99]).

Finally, it is interesting to examine the performance of the self-interaction corrected functionals for chemical shift anisotropies. Unfortunately, relatively few experimental ^{31}P chemical shift anisotropies for small, well-characterized molecules are available in the literature. Some of these values are collected in Table 7, together with results from the VWN, revPBE, SIC−VWN, and SIC−revPBE calculations. The ab initio MP2 results from the literature[6] are given for comparison. Given the small sample size, one should not attach too much significance to the average errors. Still, it appears that the SIC results follow the trend observed for the isotropic shifts. SIC−VWN performs similar to a standard GGA functional (revPBE), whereas SIC−revPBE offers a substantial improvement over both functionals. In fact, the ratio of the SIC−revPBE rms error for the shielding tensor anisotropies (41 ppm) to the total range of the experi-

TABLE 6: Statistical Evaluation of the Results for the ^{31}P NMR Chemical Shifts

molecule	VWN	revPBE	SIC−VWN	SIC−revPBE	WAH	B3LYP	MP2
All Results in Table 4 (18 Data Points)							
average abs. error, ppm	80.1	40.1	33.0	19.0			
RMS error, ppm	97.7	54.4	39.8	23.1			
correlation slope	1.156	1.069	1.036	0.950			
correlation intercept, ppm	78.0	39.2	32.5	1.0			
Excluding PBr_3, PI_3, and "P_2H_2" (15 Data Points)							
average abs. error, ppm	60.1	28.9	31.0	16.3	23.6	18.7	19.1
RMS error, ppm	69.2	36.3	35.7	20.5	27.7	25.2	27.1
correlation slope	1.076	1.008	1.025	0.980	0.970	1.036	0.970
correlation intercept, ppm	63.3	27.8	29.6	6.0	−11.5	7.2	−15.1

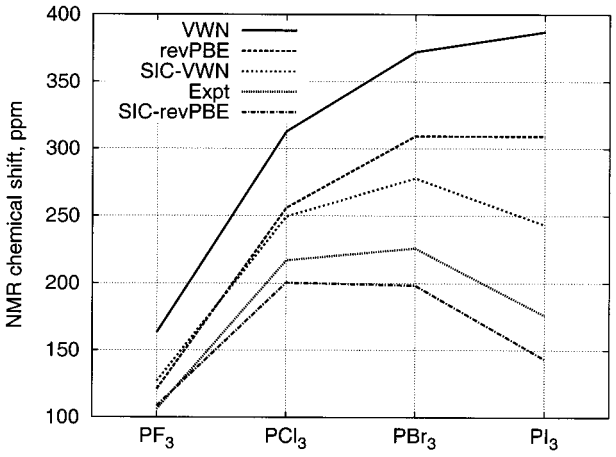

Figure 5. Correlation between calculated and experimental ^{31}P NMR chemical shifts in phosphorus(III) halides (PX_3; X = F, Cl, Br, and I).

mental anisotropies (2.3%) is almost identical to the similar ratio for the isotropic chemical shifts (2.2%). In comparison, ab initio MP2 $\Delta\sigma$ values exhibit substantial deviations from the experiment (rms error of 86 ppm) and are, in fact, comparable in quality to VWN LDA results for this property. Therefore, it appears that the excellent performance of MP2 for the isotropic ^{31}P chemical shifts arises in part from a cancellation of errors between individual components of the shielding tensors.

7. Summary and Outlook

In this work, we examined the origin of the orbital localization requirement, which is commonly postulated[43,44] in effective potential treatments of the PZ SIC. We show that the localization requirement arises from the off-diagonal Lagrangian multipliers of the coupled PZ eigenequations, which cannot be removed due to the orbital dependence of the PZ-SIC energy expression. As a consequence, orbital localization constitutes an essential component of any effective potential treatment of the PZ SIC. We also demonstrate that the ideal, energy-minimizing localization transformation is identical to the previously reported[46] energy-minimizing conditions for the solutions to the coupled PZ eigenequations. Due to the structure of this condition, it is approximately satisfied by *any* set of spatially localized orbitals, so that inexpensive localization transformations, such as Foster-Boys[79] and Pipek-Mezey[100] can be substituted for the exact conditions, with minimal loss of accuracy.

Further, we report a KLI−OEP implementation of the PZ SIC correction for gradient-corrected approximate exchange-correlation functionals within ADF. Additionally, we examine several possible approaches toward implementing frozen electron cores within the SIC−KLI−OEP technique. Molecular atomization energies are relatively insensitive to the choice of the frozen core treatment, so that all-electron results can be reproduced to within 2%, if the frozen core orbitals are simply ignored in the KLI potential expression. At the same time, Kohn−Sham orbital energies and NMR shielding constants are more sensitive to the choice of the frozen core treatment. Approximating all-electron results for these properties to within 2% requires that the frozen core orbitals are treated on an equal footing with the localized valence orbitals, during the evaluation of the KLI effective potential.

As the first application of the SIC-GGA functionals, we examine their performance for the previously studied C, H, N, O, and F NMR data set.[43] Different GGA functionals (BP86 and revPBE) lead to essentially identical results for the individual chemical shifts, when combined with the SIC. For this data set, SIC−revPBE provides a small but significant improvement for C, N, and F (rms errors: 6.5, 17.7, and 13.1 ppm, respectively), compared to the LDA-based SIC−VWN (rms errors: 7.1, 21.3, and 14.5 ppm). A similar improvement is obtained for ^{17}O chemical shifts once ozone is excluded from the statistics (SIC−VWN, 53.1; SIC-revPBE, 45.1 ppm). For the hydrogen chemical shifts, SIC−revPBE reduces the residual error by a factor of 2, compared to SIC−VWN (0.22 vs 0.44 ppm).

We further apply the SIC−revPBE functional to ^{31}P NMR chemical shifts, which are known to present a challenge for standard DFT techniques.[16] For this nucleus, the LDA-based SIC−VWN functional presents only a minor advantage over

TABLE 7: Calculated Anisotropies of the ^{31}P Shielding Tensors ($\Delta\sigma = \sigma_{\parallel} - \sigma_{\perp}$, ppm), in Comparison with the Experiment and ab Initio Theoretical Results

molecule	expt.	VWN	revPBE	SIC−VWN	SIC−revPBE	MP2[a]
P_4	−405. ± 15.[b]	−453.7	−429.4	−443.2	−416.1	−460.4
PN	1376.[c]	1578.5	1500.5	1464.6	1368.1	1222.9
PH_3	−56.0 ± 1.5[b]	−79.6	−63.2	−49.1	−41.5	−59.9
PF_3	181. ± 5[d]	247.7	237.6	275.1	262.8	275.2
$P(CH_3)_3$	7.63 ± 0.5[e]	−24.6	−21.1	−22.1	−27.2	−29.0
$OP(CH_3)_3$	173.6 ± 0.5[e]	272.5	257.0	229.3	219.3	
average abs. error, ppm[f]		75.8	48.3	51.5	30.0	68.7
RMS error, ppm[f]		99.4	63.5	61.8	40.7	85.7

[a] MP2 ab initio results are quoted from ref 6. [b] Cited from ref 106. [c] Cited from ref 6. [d] Reference 107. An alternative value of +222. ± 2. ppm was reported by the same authors previously.[108] [e] Reference 109. [f] Statistical averages exclude $OP(CH_3)_3$.

standard GGAs (revPBE rms error, 54 ppm; SIC−VWN, 40 ppm, on an 18-point data set). Most of this advantage is derived from the three "difficult" molecules in the data set (PBr_3, PI_3, and P_2H_2). At the same time, SIC−revPBE leads to an rms error of 23 ppm, or just 2.2% of the chemical shift range in the data set, with individual chemical shifts deviating from the experiment by less than 5% of the experimental shift range. Similar accuracy is maintained for SIC−revPBE NMR chemical shift anisotropies. Moreover, SIC−revPBE reproduces chemical shift trends in the PX_3 (X = F, Cl, Br, and I) series almost quantitatively. The same series is described qualitatively incorrectly by the standard LDA and GGA functionals.

In cases where comparison with other theoretical techniques is possible, SIC−revPBE ^{31}P NMR chemical shifts appear to be superior to other theoretical approaches, including B3LYP hybrid DFT calculations, ab initio MP2, and the empirically corrected WAH scheme. Overall, SIC−GGA appears to be the method of choice for the calculations of ^{31}P NMR shielding tensors in molecules with more than a few atoms.

Given the demonstrated success of self-interaction corrected DFT in prediction of the NMR shieldings of some of the "difficult" main group elements, as well as the increased applicability of the present computational implementation of the technique, several possible directions for future work are indicated. These include applications to other magnetic nuclei, calculations of reaction energies and barriers, as well as the properties accessible through time-dependent DFT. Additionally, a consistent implementation of the orbital localization condition (13) appears to be desirable, not in the least to quantify the magnitude of the error introduced because of the surrogate localization conditions used presently. Other methodological developments may include incorporation of SIC within a spin−orbit coupling scheme, as well as support for a more robust relativistic treatment, such as ZORA.[101,102] In this respect, it is interesting to note that the time-independent relativistic extension of the KLI−OEP potential is formally identical to the corresponding nonrelativistic expression,[103] so that scalar ZORA support can be incorporated within the existing program with a minimal effort. Work along these lines is currently in progress.

Acknowledgment. This work has been supported by the National Sciences and Engineering Research Council of Canada (NSERC), as well as by the donors of the Petroleum Research Fund, administered by the American Chemical Society (ACS-PRF No. 36543-AC3). S.P. acknowledges Dr. Jochen Autschbach for helpful discussions.

Supporting Information Available: Slater-type triple-ζ polarized basis sets, optimized for SIC calculations for C, N, O, F, P, Si, Cl, Cr, Br, and I. Optimized molecular geometries of the phorphorus reference set. Calculated SIC−BP86 and SIC−revPBE chemical shifts for the C, H, N, O, and F reference set (26 pages). This material is available free of charge via the Internet at http://pubs.acs.org.

References and Notes

(1) Mason, J., Ed.; *Multinuclear NMR*; Plenum: New York, 1987.
(2) Picard, F.; Paquet, M. J.; Levesque, J.; Belanger, A.; Auger, M. *Biophys. J.* **2000**, *77*, 888.
(3) Richter, C.; Reif, B.; Griesinger, C.; Schwalbe, H. *J. Am. Chem. Soc.* **2000**, *122*, 12728.
(4) Wu, Z.; Tjandra, N.; Bax, A. *J. Am. Chem. Soc.* **2001**, *123*, 3617.
(5) Kutzelnigg, W.; Fleischer, U.; Schindler, M. *NMR* **1990**, *23*, 165.
(6) Chesnut, D. B.; Byrd, E. F. C. *Heteroatom Chem.* **1996**, *7*, 307.
(7) Kaupp, M. *Chem. Ber.* **1996**, *129*, 535.
(8) Chesnut, D. B.; Quin, L. D. *Heteroatom Chem.* **1997**, *8*, 451.
(9) Alkorta, I.; Elguero, J. *Struct. Chem.* **1998**, *9*, 187.
(10) Dransfeld, A.; Chesnut, D. B. *Chem. Phys.* **1998**, *234*, 69.
(11) Ruiz-Moralez, Y.; Ziegler, T. *J. Phys. Chem. A* **1998**, *102*, 3970.
(12) Dransfeld, A.; Schleyer, P.v. R. *Magn. Res. Chem.* **1998**, *36*, S29.
(13) Chesnut, D. B.; Quin, L. D. *Heteroatom Chem.* **1999**, *10*, 566.
(14) Kaupp, M.; Aubauer, C.; Engelhardt, G.; Klapötke, T. M.; Malkina, O. L. *J. Chem. Phys.* **1999**, *110*, 3897.
(15) Bühl, M.; Kaupp, M.; Malkina, O. L.; Malkin, V. G. *J. Comput. Chem.* **1999**, *20*, 91.
(16) van Wüllen, C. *Phys. Chem. Chem. Phys.* **2000**, *2*, 2137.
(17) Wosnick, J. H.; Morin, F. G.; Gilson, D. F. R. *Can. J. Chem.* **1998**, *76*, 1280.
(18) Gauss, J. *Chem. Phys. Lett.* **1992**, *191*, 614.
(19) Gauss, J. *J. Chem. Phys.* **1993**, *99*, 3629.
(20) Kollwitz, M.; Gauss, J. *Chem. Phys. Lett.* **1996**, *260*, 639.
(21) Cybulski, S. M.; Bishop, D. M. *J. Chem. Phys.* **1997**, *106*, 4082.
(22) Gauss, J.; Stanton, J. F. *J. Chem. Phys.* **1995**, *103*, 3561.
(23) Gauss, J.; Stanton, J. F. *J. Chem. Phys.* **1996**, *104*, 2574.
(24) Christiansen, O.; Gauss, J.; Stanton, J. F. *Chem. Phys. Lett.* **1997**, *266*, 53.
(25) Hansen, A. E.; Bouman, T. D. In *Nuclear Magnetic Shieldings and Molecular Structure*; Tossell, J. A., Ed.; Kluwer: Dordrecht, The Netherlands, 1993; pp 117−140.
(26) Kutzelnigg, W.; van Wüllen, C.; Fleischer, U.; Franke, R.; Mourik, T. v. In *Nuclear Magnetic Shieldings and Molecular Structure*; Tossell, J. A., Ed.; Kluwer: Dordrecht, The Netherlands, 1993; pp 141−161.
(27) van Wüllen, C.; Kutzelnigg, W. *J. Chem. Phys.* **1996**, *104*, 2330.
(28) Malkin, V. G.; Malkina, O. L.; Salahub, D. R. *Chem. Phys. Lett.* **1993**, *204*, 80.
(29) Malkin, V. G.; Malkina, O. L.; Casida, M. E.; Salahub, D. R. *J. Am. Chem. Soc.* **1994**, *116*, 5898.
(30) Malkin, V. G.; Malkina, O. L.; Erikson, L. A.; Salahub, D. R. *Theoretical and Computational Chemistry, Vol. 2*; Seminario, J. M., Politzer, P., Eds.; Elsevier: Amsterdam, 1995.
(31) Schreckenbach, G.; Ziegler, T. *J. Phys. Chem.* **1995**, *99*, 606.
(32) Lee, A. M.; Handy, N. C.; Colwell, S. M. *J. Chem. Phys.* **1995**, *103*, 10095.
(33) Cheeseman, J. R.; Trucks, G. W.; Keith, T. A.; Frisch, M. J. *J. Chem. Phys.* **1996**, *104*, 5497.
(34) Rauhut, G.; Puyear, S.; Wolinski, K.; Pulay, P. *J. Phys. Chem.* **1996**, *100*, 6310.
(35) Schreckenbach, G.; Ziegler, T. *Int. J. Quantum Chem.* **1997**, *61*, 899.
(36) Wilson, P. J.; Amos, R. D.; Handy, N. C. *Chem. Phys. Lett.* **1999**, *312*, 475.
(37) Helgaker, T.; Wilson, P. J.; Amos, R. D.; Handy, N. C. *J. Chem. Phys.* **2000**, *113*, 2983.
(38) Malkin, V. G.; Malkina, O. L.; Salahub, D. R. *Chem. Phys. Lett.* **1993**, *204*, 87.
(39) Olsson, L.; Cremer, D. *J. Phys. Chem.* **1996**, *100*, 16881.
(40) Olsson, L.; Cremer, D. *J. Chem. Phys.* **1996**, *105*, 8995.
(41) van Wüllen, C. *J. Chem. Phys.* **1995**, *102*, 2806.
(42) Helgaker, T.; Watson, M.; Handy, N. C. *J. Chem. Phys.* **2000**, *113*, 9402.
(43) Patchkovskii, S.; Autschbach, J.; Ziegler, T. *J. Chem. Phys.* **2001**, *115*, 26.
(44) Garza, J.; Nichols, J. A.; Dixon, D. A. *J. Chem. Phys.* **2000**, *112*, 7880.
(45) Perdew, J. P.; Zunger, A. *Phys. Rev. B* **1981**, *23*, 5048.
(46) Whitehead, M. A. In *Recent Advances in Density Functional Methods, Part II*; Chong, D. P., Ed.; World Scientific: Singapore, 1997.
(47) Goedecker, S.; Umrigar, C. J. *Phys. Rev. A* **1997**, *55*, 1765.
(48) Sharp, R. T.; Horton, G. K. *Phys. Rev.* **1953**, *90*, 317.
(49) Talman, J. D.; Shadwick, W. F. *Phys. Rev. A* **1970**, *14*, 36.
(50) Krieger, J. B.; Li, Y.; Iafrate, G. J. *Phys. Rev. A* **1992**, *45*, 101.
(51) Krieger, J. B.; Li, Y.; Iafrate, G. J. *Phys. Rev. A* **1992**, *46*, 5453.
(52) Li, Y.; Krieger, J. B.; Iafrate, G. J. *Phys. Rev. A* **1993**, *47*, 165.
(53) Engel, E.; Dreizler, R. M. *J. Comput. Chem.* **1999**, *20*, 31.
(54) Pederson, M. R.; Heaton, R. A.; Lin, C. C. *J. Chem. Phys.* **1984**, *80*, 1972.
(55) Pederson, M. R.; Heaton, R. A.; Lin, C. C. *J. Chem. Phys.* **1985**, *82*, 2688.
(56) te Velde, G.; Bickelhaupt, F. M.; Baerends, E. J.; Fonseca Guerra, C.; van Gisbergen, S. J. A.; Snijders, J. G.; Ziegler, T. *J. Comput. Chem.* **2001**, *22*, 931.
(57) Ullrich, C. A.; Reinhard, P.-G.; Suraud, E. *Phys. Rev. A* **2000**, *62*, 053202.
(58) Hirata, S.; Ivanov, S.; Grabowski, I.; Bartlett, R. J.; Burke, K.; Talman, J. D. *J. Chem. Phys.* **2001**, *115*, 1635.
(59) Ivanov, S.; Bartlett, R. J. *J. Chem. Phys.* **2001**, *114*, 1952.
(60) Ziegler, T. *Chem. Rev.* **1991**, *91*, 651.
(61) Perdew, J. P.; Ernzerhof, M. In *Electronic Density Functional Theory: Recent Progress and New Directions*; Dobson, J. F., Vignale, G., Das, M. P., Eds.; Plenum: New York, 1998.

(62) Salahub, D. R.; Castro, M.; Proynov, E. Y. In *Relativistic and Electron Correlation Effects in Molecules and Solids*; Malli, G. L., Ed.; Plenum: New York, 1994.
(63) Poole, C. P., Jr. *The Physics Handbook*; Wiley: New York, 1998.
(64) Baerends, E. J.; Ellis, D. E.; Ros, P. *Chem. Phys.* **1973**, *2*, 41.
(65) Fonseca Guerra, C.; Visser, O.; Snijders, J. G.; te Velde, G.; Baerends, E. J. In *Methods and Techniques in Computational Chemistry METECC-95*; Clementi, E., Corongiu, C., Eds.; STEF: Cagliari, 1995.
(66) Garza, J.; Vargas, R.; Nichols, J. A.; Dixon, D. A. *J. Chem. Phys.* **2001**, *114*, 639.
(67) Landau, L. D.; Lifshitz, E. M. *Quantum Mechanics. Nonrelativistic Theory*; Pergamon: Oxford, U.K., 1977.
(68) Parr, R. G.; Yang, W. *Density Functional Theory of Atoms and Molecules*; Oxford University Press: Oxford, U.K., 1989.
(69) *ADF*, version 2.3.3; Department of Theoretical Chemistry, Vrije Universiteit: Amsterdam; http://tc.chem.vu.nl/SCM.
(70) te Velde, G.; Baerends, E. J. *J. Comput. Chem.* **1992**, *9*, 84.
(71) Versluis, L.; Ziegler, T. *J. Chem. Phys.* **1988**, *88*, 322.
(72) Perdew, J. P.; Burke, K.; Ernzerhof, M. *Phys. Rev. Lett.* **1996**, *77*, 3865.
(73) Zhang, Y.; Yang, W. *Phys. Rev. Lett.* **1998**, *80*, 890.
(74) Patchkovskii, S. *Self-Consistent Implementation of Perdew-Burke-Ernzerhof and related GGAs in ADF*. Technical Report; Department of Chemistry, University of Calgary: Calgary, 2000.
(75) All standard ADF basis sets are available on the Internet at http://www.scm.com/Doc/atomicdata/.
(76) Ziegler, T.; Tschinke, V.; Baerends, E. J.; Snijders, J. G.; Ravenek, W. *J. Phys. Chem.* **1989**, *93*, 3050.
(77) Galy, J.; Enjalbert, R. *J. Solid State Chem.* **1982**, *44*, 1.
(78) Kuchitsu, K., Ed.; *Landolt-Börnstein, Group II: Molecules and Radicals*; Springer: Berlin, 1995; Vols. 7, 15, 21, and 23.
(79) Foster, J. M.; Boys, S. F. *Rev. Mod. Phys.* **1960**, *32*, 300.
(80) Autschbach, J. *Lokalisierte Molekülorbitale mit dem Amsterdam Density Functional Programm*, Diplomarbeit; Universität Siegen: Siegen, 1996.
(81) London, F. *J. Phys. Rad.* **1937**, *8*, 397.
(82) Hameka, H. F. *Mol. Phys.* **1958**, *1*, 203.
(83) Ditchfield, R. *Mol. Phys.* **1974**, *27*, 789.
(84) Schreckenbach, G.; Ziegler, T. *Theor. Chem. Acc.* **1998**, *99*, 71.
(85) Patchkovskii, S.; Ziegler, T. to be published.
(86) Vosko, S. H.; Wilk, L.; Nusair, M. *Can. J. Phys.* **1980**, *58*, 1200.
(87) Becke, A. D. *Phys. Rev. A* **1988**, *38*, 3098.
(88) Perdew, J. P. *Phys. Rev. B* **1986**, *33*, 8822; **1986**, *34*, 7406.
(89) Helgaker, T.; Jaszunski, M.; Ruud, K. *Chem. Rev.* **1999**, *99*, 293.
(90) Coriani, S.; Jaszuński, M.; Rizzo, A.; Ruud, K. *Chem. Phys. Lett.* **1998**, *287*, 677.
(91) Rablen, P. R.; Pearlman, S. A.; Finkbiner, J. *J. Phys. Chem. A* **1999**, *103*, 7357.
(92) Sundholm, D.; Gauss, J.; Schäfer, A. *J. Chem. Phys.* **1996**, *105*, 11051.
(93) Chesnut, D. B. *Chem. Phys.* **1997**, *214*, 73.
(94) Ruud, K.; Åstrand, P.-O.; Taylor, P. R. *J. Am. Chem. Soc.* **2000**, *123*, 4826.
(95) Jameson, C. J.; de Dios, A.; Jameson, A. K. *Chem. Phys. Lett.* **1990**, *167*, 575.
(96) Wolff, S. K.; Ziegler, T. *J. Chem. Phys.* **1998**, *109*, 895.
(97) Vaara, J.; Malkina, O. L.; Stoll, H.; Malkin, V. G.; Kaupp, M. *J. Chem. Phys.* **2001**, *114*, 61.
(98) Fukawa, S.; Hada, M.; Fukuda, R.; Tanaka, S.; Nakatsuji, H. *J. Comput. Chem.* **2001**, *22*, 528.
(99) Zilm, K. W.; Webb, G. G.; Cowley, A. H.; Pakulski, M.; Orendt, A. *J. Am. Chem. Soc.* **1988**, *110*, 2032.
(100) Pipek, J.; Mezey, P. G. *J. Chem. Phys.* **1989**, *90*, 4916.
(101) Chang, C.; Pelissier, M.; Durand, M. *Phys. Scr.* **1986**, *34*, 394.
(102) van Lenthe, E.; Baerends, E. J.; Snijders, J. G. *J. Chem. Phys.* **1993**, *99*, 4597.
(103) Kreibich, T.; Gross, E. K. U.; Engel, E. *Phys. Rev. A* **1998**, *57*, 138.
(104) Tattershall, B. W.; Kendall, N. L. *Polyhedron* **1994**, *13*, 1517.
(105) Dillon, K. B.; Dillon, M. G. C.; Waddington, T. C. *J. Inorg. Nucl. Chem.* **1976**, *38*, 1149.
(106) Jameson, C. J.; Jameson, A. K.; Burrell, P. M. *J. Chem. Phys.* **1980**, *73*, 6013.
(107) Montana, A. J.; Zumbulyadis, N.; Dailey, B. P. *J. Chem. Phys.* **1976**, *65*, 4756.
(108) Zumbulyadis, N.; Dailey, B. P. *Mol. Phys.* **1973**, *26*, 3.
(109) Montana, A. J.; Zumbulyadis, N.; Dailey, B. P. *J. Am. Chem. Soc.* **1977**, *99*, 4290.